

Shear Modulus of Two-Dimensional Foams: the Effect of Area Dispersity and Disorder

S.J. Cox^a and E.L. Whittick

Institute of Mathematical and Physical Sciences, University of Wales Aberystwyth, Ceredigion SY23 3BZ, UK.

Abstract. We use the Surface Evolver to determine the shear modulus G of a dry 2D foam of 2500 bubbles, using both extensional and simple shear. We examine G for a range of monodisperse, bidisperse and polydisperse foams, and relate it to various measures of the structural disorder of each foam. In all cases, the shear modulus of a foam decreases with increasing disorder.

PACS. 47.57.Bc Foams and Emulsions – 83.80.Iz Emulsions and Foams – 83.50.Jf Extensional flow and combined shear and extension

1 Introduction

An aqueous foam is collection of gas bubbles contained within a continuous liquid network [1]. Despite its fluid composition, it shows an elastic response at low strains, more usually associated with solids. At higher strains, topological changes occur in the bubble structure, leading to plastic deformation and yielding. Here we study the shear modulus of these complex fluids, which characterizes the elastic response, and show how it depends upon the disordered structure of the foam.

Princen's [2] calculation of the shear modulus of a hexagonal 2D dry foam is the basis for this work. The small-strain, static shear modulus G is defined for simple shear by

$$G = \left. \frac{d\tau_{xy}}{d\epsilon} \right|_{\epsilon=0} \quad (1)$$

^a Email: foams@aber.ac.uk

where τ_{xy} is the shear stress and ϵ the strain. Here, we restrict to the dry limit, so the shear modulus of a hexagonal foam of bubbles with area A can be written directly in terms of the surface tension of the films, γ , and either the radius R of a circle of equivalent area or the length L of the sides of the hexagons:

$$G_{hex} = \sqrt{\frac{\sqrt{3}}{2\pi}} \frac{\gamma}{R} = \frac{1}{\sqrt{3}} \frac{\gamma}{L} = \sqrt{\frac{\sqrt{3}}{2}} \frac{\gamma}{\sqrt{A}} \quad (2)$$

This result provides a fair estimate of the shear modulus of many disordered 2D foams, and is in fact exact for any *polydisperse* hexagonal system [3], with L and A replaced by their system-wide averages \bar{L} and \bar{A} .

Here, we show how (2) must be modified to allow the accurate prediction of the shear modulus of disordered 2D foams, including those that are bidisperse or polydisperse in bubble area.

Kruyt [4] recently gave a number of micro-mechanical predictions for G which depend upon

the distributions of bubble areas and edge lengths. Although that work included comparison with a simulation, our motivation here is in part to provide comprehensive data to improve models of this kind, and we evaluate the success of these models in relation to our data below.

Previous numerical work on calculating shear moduli for 2D foams is summarised in [5], for periodic foams in both simple and extensional shear. In addition, Weaire et al. [6] show that G decreases with increasing disorder in the number of sides, based upon 64-bubble polydisperse foams under extensional shear. These authors conjectured that no 2D monodisperse foam has higher shear modulus than the hexagonal honeycomb, and Kraynik et al. [3] extended this conjecture to polydisperse hexagonal systems.

However, we can find little systematic data measuring shear modulus as a function of structural disorder, although such work does exist for 3D foams [7, 8]. Yet 2D foams, such as those squeezed between glass plates, are still of interest. They provide a simple system for the study of rheology, where benefits include the possibility to measure the deformation and position of each constituent element (bubbles) over time.

We first describe the creation of the foam structures, then analyse their structural statistics at equilibrium in §3. In §4 we calculate three values of shear modulus for each foam and discuss the variation of the average with disorder.

2 Foam Creation

We use the Surface Evolver [9] in circular arc mode, so that all edges are accurately represented as arcs of circles. Foams are generated using a Voronoi procedure based upon randomly scattered (Poisson) points. The foam samples are periodic with total area equal to one and the $N = 2500$ bubbles

each have fixed area, which is set as part of the initialization of the structure.

For each foam we first find a minimum of the total edge length E (equivalent to energy when multiplied by surface tension γ , which is here taken equal to 2), allowing T1 neighbour-switching events [10] where an edge length shrinks below a critical value. This critical value is randomly chosen in the range [0.001 : 0.004], where the upper limit is effectively fixed by the condition that no T1s must occur during shearing - it is about one-third of the average edge length.

Each sample is then annealed to drive the foam towards a deeper energetic minimum by applying large amplitude simple shear deformations to trigger T1 events, with the aim of creating isotropic structures that are more representative of real foams. (Extension-compression cycles, as used by Kraynik et al. [7] in 3D, lead to a high degree of anisotropy, and were therefore avoided). Step strains of $+1/4$, $-1/4$, $-1/4$ and $+1/4$ are performed in the xy direction, with edge-length minimising iterations between each step, and then repeated in the yx direction. Both cycles are repeated five times, and then the foam is converged to equilibrium, performing T1s where necessary.

The components of stress $\underline{\underline{\tau}}$ are found by integrating the tension forces along each edge [11]:

$$\underline{\underline{\tau}} = \gamma \int_{edges} \underline{t} \otimes \underline{t} dL, \quad (3)$$

where \underline{t} denotes the tangent to the edge. Note that the total area of the foam is set to one. For the special case of the circular arcs used here, we first calculate the radius of curvature R_c of each edge and then the orientations θ_1 and θ_2 of its endpoints.

Then

$$\begin{aligned} \begin{pmatrix} \tau_{xx} & \tau_{xy} \\ \tau_{yx} & \tau_{yy} \end{pmatrix} &= \gamma \sum_{edges} \int_{\theta_1}^{\theta_2} \begin{pmatrix} \cos^2 \theta & \cos \theta \sin \theta \\ \cos \theta \sin \theta & \sin^2 \theta \end{pmatrix} R_c d\theta \\ &= \gamma \sum_{edges} \frac{R_c}{2} \begin{pmatrix} \Delta_+ & \Delta^2 \\ \Delta^2 & \Delta_- \end{pmatrix} \end{aligned} \quad (4)$$

where

$$\Delta_{\pm} = \theta_2 - \theta_1 \pm \cos(\theta_1 + \theta_2) \sin(\theta_2 - \theta_1) \quad (5)$$

and

$$\Delta^2 = \cos^2 \theta_1 - \cos^2 \theta_2. \quad (6)$$

The sample is sheared in order to reduce the off-diagonal component τ_{xy} and the normal stress $\tau_{xx} - \tau_{yy}$ towards zero. Simple shear is applied first, until $|\tau_{xy}| < 0.02$, and then extensional strain is applied, until $|\tau_{xx} - \tau_{yy}| < 0.1$, and the cycle repeated. The energy of the sample is again reduced to its minimum value. This represents the starting point for the calculation of shear modulus.

2.1 Disorder

The disorder of the foam, irrespective of the distribution of bubble areas, is measured through the second moment of the distribution of the number of sides of each bubble:

$$\mu_2(n) = \sum_n p(n)(n-6)^2 \quad (7)$$

where $p(n)$ is the fraction of bubbles with n sides. The result of annealing the foam is to reduce the value of $\mu_2(n)$.

Further measures of disorder include the second moment of the area distribution:

$$\mu_2(A) = \overline{\left(\frac{A}{\bar{A}} - 1\right)^2}, \quad (8)$$

where the bar denotes averaging ($\bar{A} = 0.0004$ is the average bubble area), and the second moment of the edge length distribution:

$$\mu_2(L) = \overline{\left(\frac{L}{\bar{L}} - 1\right)^2}. \quad (9)$$

The total perimeter of the foam, E , gives the average edge length, $\bar{L} = E/(3N)$

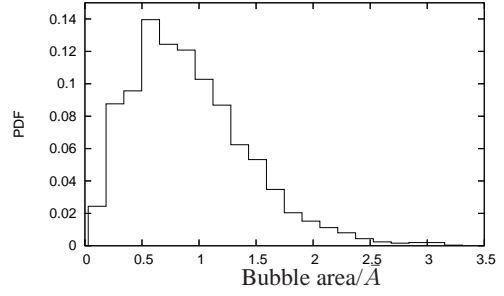


Fig. 2. Histogram (21 bins) of normalised bubble areas for the polydisperse foam in figure 1(d).

We examine over 180 different, disordered, foams, and first categorise them according to the dispersity in bubble areas. Examples of the foams simulated are shown in figure 1. A coordinate system (x, y) is defined to be parallel to the edges of the unit cell.

The samples arising from the Voronoi procedure are naturally polydisperse (figure 1(d)). A typical area distribution is shown in figure 2.

We make disordered *monodisperse* foams (figure 1(a)) by equating the areas of the bubbles in a polydisperse foam, so that $A = \bar{A} = 0.004$.

Bidisperse foams with area ratio $a_r = 0.2, 0.3, \dots, 0.8$ were formed from a polydisperse sample by assigning those bubbles with area greater than the average (about 45%) to have area A_1 and the rest to have area $A_2 = a_r A_1$, then scaled to have the sum of the areas equal to one. Examples are shown in figure 1(b) and (c). The parameter a_r is related to the disorder parameter $\mu_2(A)$ according to

$$\mu_2(A) = \frac{k + (1-k)a_r^2}{(k + (1-k)a_r)^2} - 1 \quad (10)$$

where k is the proportion of bubbles with area A_1 , here about 0.45. Thus low a_r corresponds to large $\mu_2(A)$ and vice versa, with $a_r = 1$ denoting monodispersity. In this case, it is also straightforward to relate a_r to alternative measures of area disorder, such as $R_{21} = \langle R^2 \rangle / \langle R \rangle = 1/\sqrt{\pi} \sum A_i / \sum \sqrt{A_i}$, where R is the equivalent circle radius.

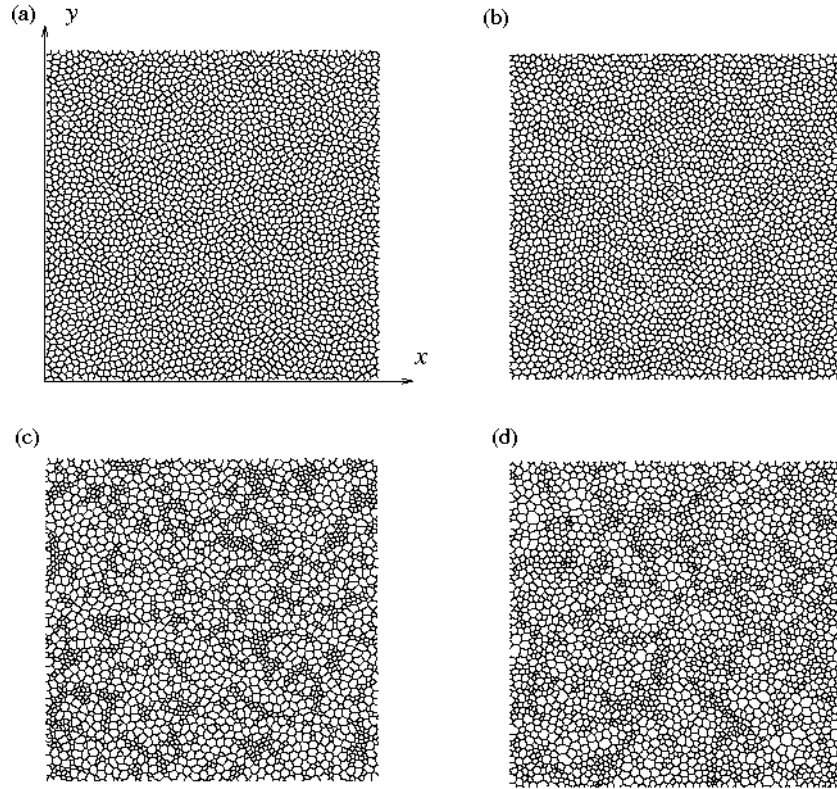


Fig. 1. Examples of the 2D periodic foams considered here, defining the x and y coordinate axes. (a) Monodisperse foam, with $\mu_2(n) = 0.511$. (b) Bidisperse, with $a_r = 0.7$, $\mu_2(n) = 0.454$ and $\mu_2(A) = 0.032$. (c) Bidisperse, with $a_r = 0.3$, $\mu_2(n) = 1.174$ and $\mu_2(A) = 0.329$. (d) Polydisperse, with $\mu_2(n) = 0.989$ and $\mu_2(A) = 0.263$. These foams are taken as representative whenever specific distributions are required in the following.

3 Structure

We compare the values of $\mu_2(n)$, $\mu_2(A)$ and $\mu_2(L)$ for these different foams in figure 3, and examine how the average edge length varies with each of these parameters in figure 4 (recall that the average area is constant). Precise correlations are hard to find, however. Recall the example of a polydisperse hexagonal foam, which has area disorder ($\mu_2(A)$ non-zero) but no disorder in the number of sides ($\mu_2(n) = 0$). Here, we have the opposite: monodisperse foams, with no area disorder, show a range of values of $\mu_2(n)$.

Monodisperse foams span a range in $\mu_2(n)$ of about 0.3, which reflects the range of critical lengths used to trigger T1 events in the foam's evolution,

and within this range $\mu_2(L)$ increases linearly. As the area-ratio a_r of a bidisperse foam is reduced, the value of $\mu_2(L)$ at given $\mu_2(n)$ decreases. On average, however, there is an increase of $\mu_2(L)$ with decreasing a_r , reflecting the increase in $\mu_2(n)$ with increasing area dispersity. For each value of a_r the data span a range in $\mu_2(n)$ of about 0.3, as for monodisperse foams. Polydisperse foams are clustered around $\mu_2(n) = 1.2$, $\mu_2(A) = 0.3$ and $\mu_2(L) = 0.13$, with no clear trends emerging.

The average edge length of a foam spans a narrow range for given $\mu_2(A)$, and decreases linearly from above the honeycomb value. For given area dispersity, \bar{L} increases almost linearly with $\mu_2(n)$. For polydisperse foams, the value of \bar{L} is always close to 0.0122.

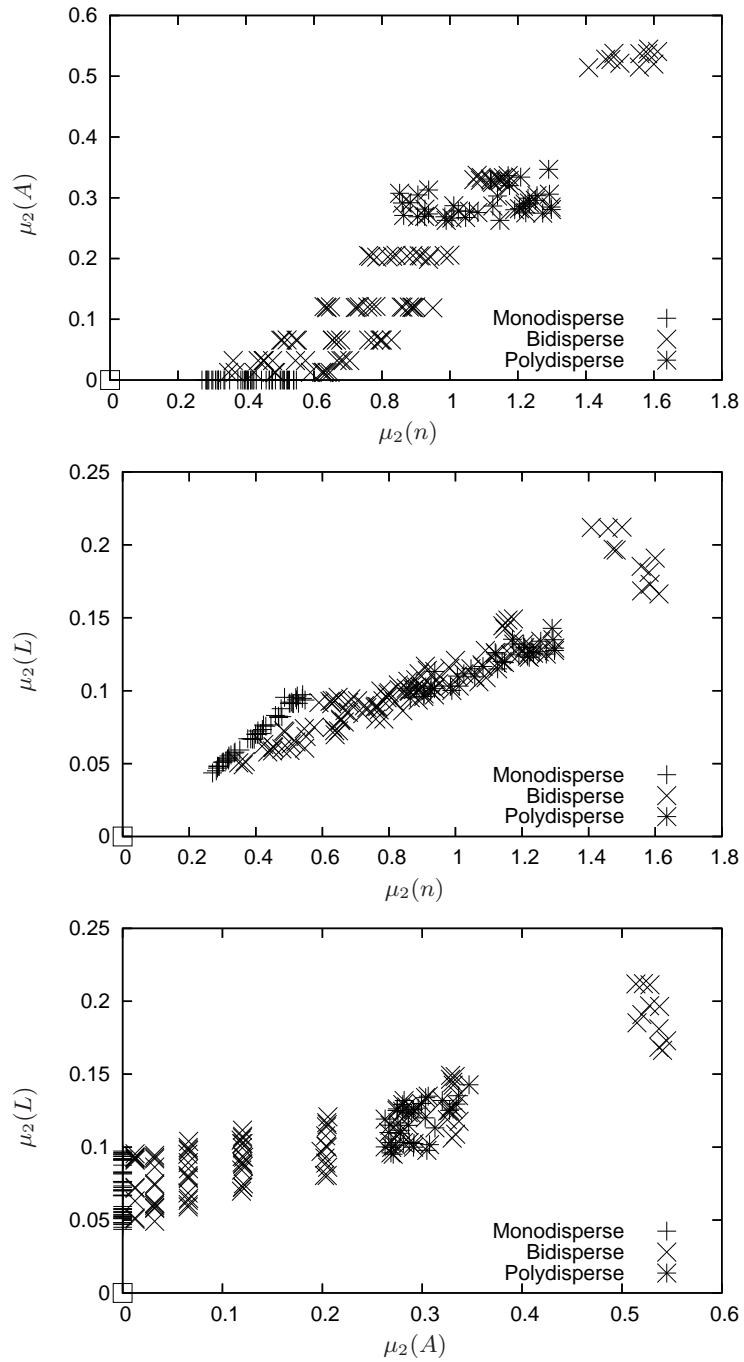


Fig. 3. Comparison of the disorder parameters. The largest values of each disorder parameter are found for bidisperse foams with small area ratio. The honeycomb values are given by open squares.

Starting from a regular hexagonal foam, we performed a single T1 and re-equilibrated the structure to find the difference in average edge length: $\Delta\bar{L} = 0.01416/(3N)$. This allows us to give a prediction of the increase in edge length with disorder (cf [12, eq. 20]) in a monodisperse foam:

$$\begin{aligned}\bar{L} &= \sqrt{\frac{2\bar{A}}{3\sqrt{3}}} + \frac{\Delta\bar{L}}{\Delta\mu_2(n)}\mu_2(n) \\ &= 0.620\sqrt{\bar{A}} + 0.00118\mu_2(n).\end{aligned}\quad (11)$$

This line overestimates (see figure 4) the average edge length when there is greater disorder.

The distributions of edge orientations and lengths are also calculated for each foam. The orientation θ of a edge is defined as the angle that the line joining the end points of the edge makes with the x -direction, in the range $[0, \pi]$. For a fully isotropic structure, the distribution of orientations θ should be constant, but as figure 5(a) shows this is not quite the case for these foams, despite the use of periodic boundary conditions to eliminate edge effects.

The distribution of normalized edge lengths is shown in figure 5(b). As the area disorder increases, the peak of the distribution decreases below one and a tail develops, indicating that a few longer edges appear. Here, the honeycomb case would give a delta function at $L/\bar{L} = 1$.

4 Shear Modulus

We now seek the value of G as a function of the disorder parameters, $G(\mu_2(n), \mu_2(A), \mu_2(L))$. For the honeycomb we have $G_{hex} = \gamma\sqrt{\sqrt{3}/(2A)} = 0.931\gamma/\sqrt{A}$, from (2), which provides a reference state at $\mu_2(n) = \mu_2(A) = \mu_2(L) = 0$.

The shear modulus is calculated in three ways, described below, with a strain of $\epsilon = 0.0005$ throughout. We checked that the results do not depend upon this value of epsilon, and that no T1s occur during the quasi-static evolution.

The stress $\underline{\underline{\tau}}^0$ in the rest state ($\epsilon = 0$) is first recorded. Then the unit cell is sheared in the xy direction and the shear modulus

$$G_{xy} = \frac{\tau_{xy} - \tau_{xy}^0}{\epsilon}, \quad (12)$$

is found. The foam is returned to the rest state, re-converged, and then sheared in the yx direction to give a value G_{yx} . The foam is again returned to the rest state and re-converged, and then an extensional strain step in the xx direction is performed to give [1, 4]

$$G_{xx} = \frac{(\tau_{xx} - \tau_{yy}) - (\tau_{xx}^0 - \tau_{yy}^0)}{4\epsilon}. \quad (13)$$

Finally, a simple average is taken of these three values.

Although for an isotropic medium all three should be the same [13], the variation in G is further evidence of the slight anisotropy of the foams. However, an error bar drawn from the smallest to the largest value of G is still smaller than the point size in figure 6, so they are omitted.

Figure 6 shows that scaling the shear modulus purely on the basis of the average bubble area does not give a high degree of accuracy. The values of G are all below the honeycomb value and differ by up to 12%.

In general, G decreases almost linearly with increasing side number disorder, $\mu_2(n)$. Bidisperse foams have a shear modulus that decreases from the honeycomb value with increasing disorder in the number of sides n , the bubble areas, and the edge lengths L . Here, the most disordered foams are the bidisperse ones with $a_r = 0.2$. Polydisperse foams are clustered in a fairly narrow range of G around 0.84, and within that range there is not a clear trend. They show the lowest shear moduli for given disorder.

The clearest correlation is that between $\mu_2(n)$ and G : roughly $G = G_{hex} - 3.95\gamma\mu_2(n)/\sqrt{A}$. It is a sharper decrease than that of Weaire et al. [6], who find $G \approx G_{hex} - 2.2\gamma\mu_2(n)/\sqrt{A}$. The ratio

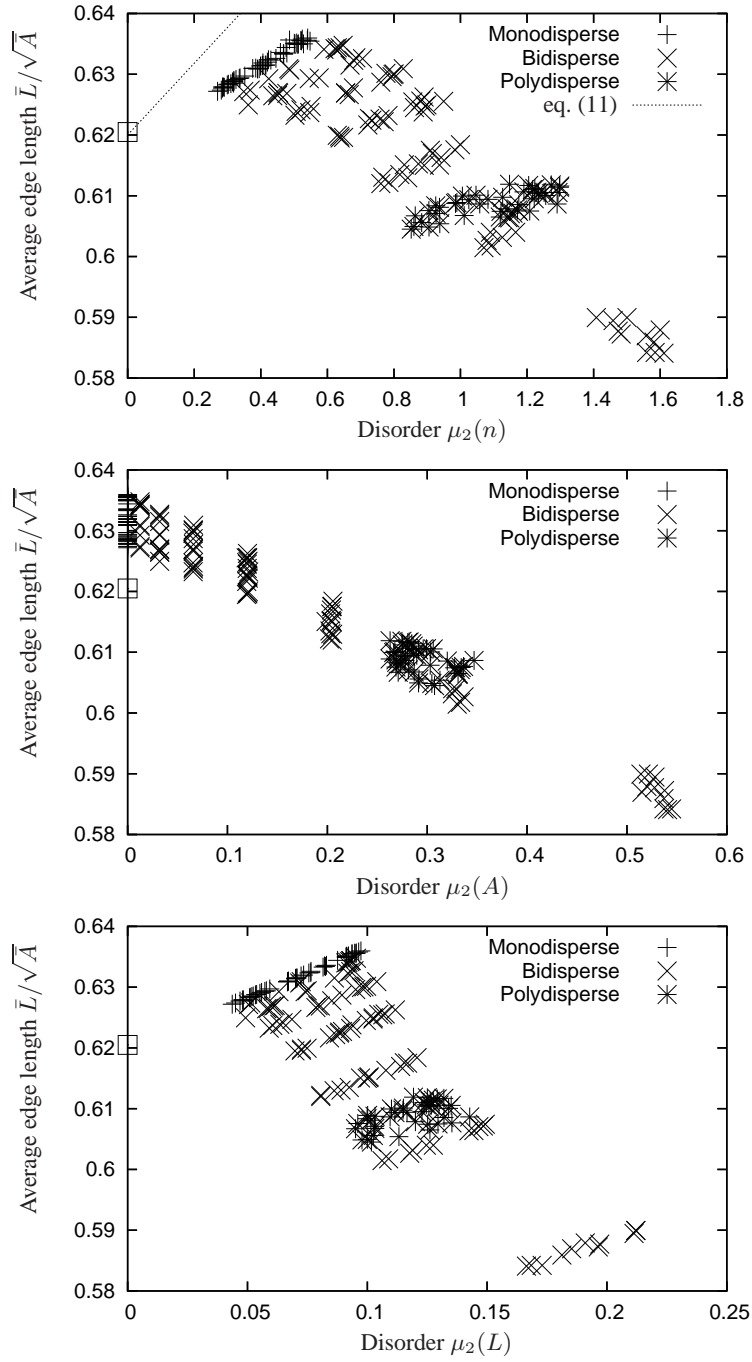


Fig. 4. The average edge length, normalized by $\sqrt{A} = 0.02$, versus each of the disorder parameters. Here the honeycomb value does not provide a lower bound.

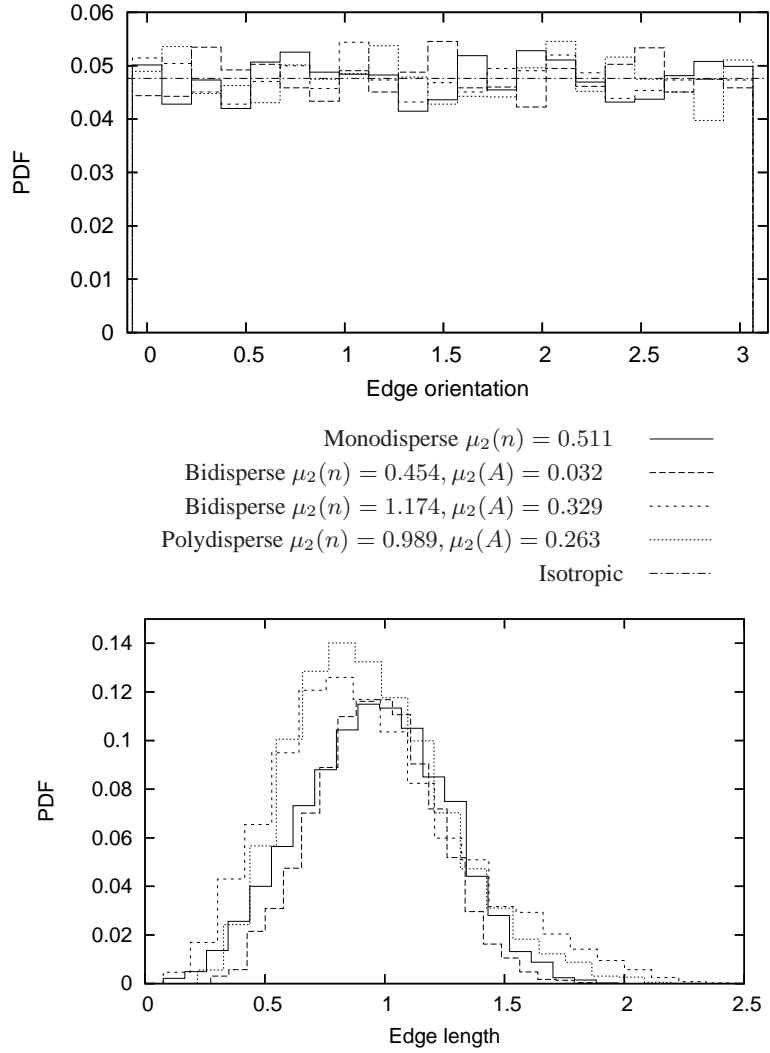


Fig. 5. (a) Representative histograms (21 bins) of edge orientation show that a monodisperse foam has the greatest deviation from the isotropic case, while a polydisperse foam is within 20% of the isotropic value. (b) In the case of edge length (normalized by average edge length), there is a subtle change in the distribution as $\mu_2(A)$ increases: the peak in edge length becomes higher and a tail appears.

of foam energy to shear modulus, shown in figure 7, is above the honeycomb value and increases slightly with increasing $\mu_2(n)$.

The shear modulus appears to stop decreasing at high disorder, corresponding to bidisperse foams with small area ratio a_r . This effect may be attributable to the decoration of a foam of large bubbles with small bubbles, which does not change G ; in the ordered case of a hexagonal foam deco-

rated with a small three-sided bubble at each three-fold vertex, G should decrease by a factor of $\sqrt{3}$ from the honeycomb value [6, 3].

The following micro-mechanical predictions of G , due to Kruyt [4], are based upon the distributions of bubble areas and edge lengths respec-

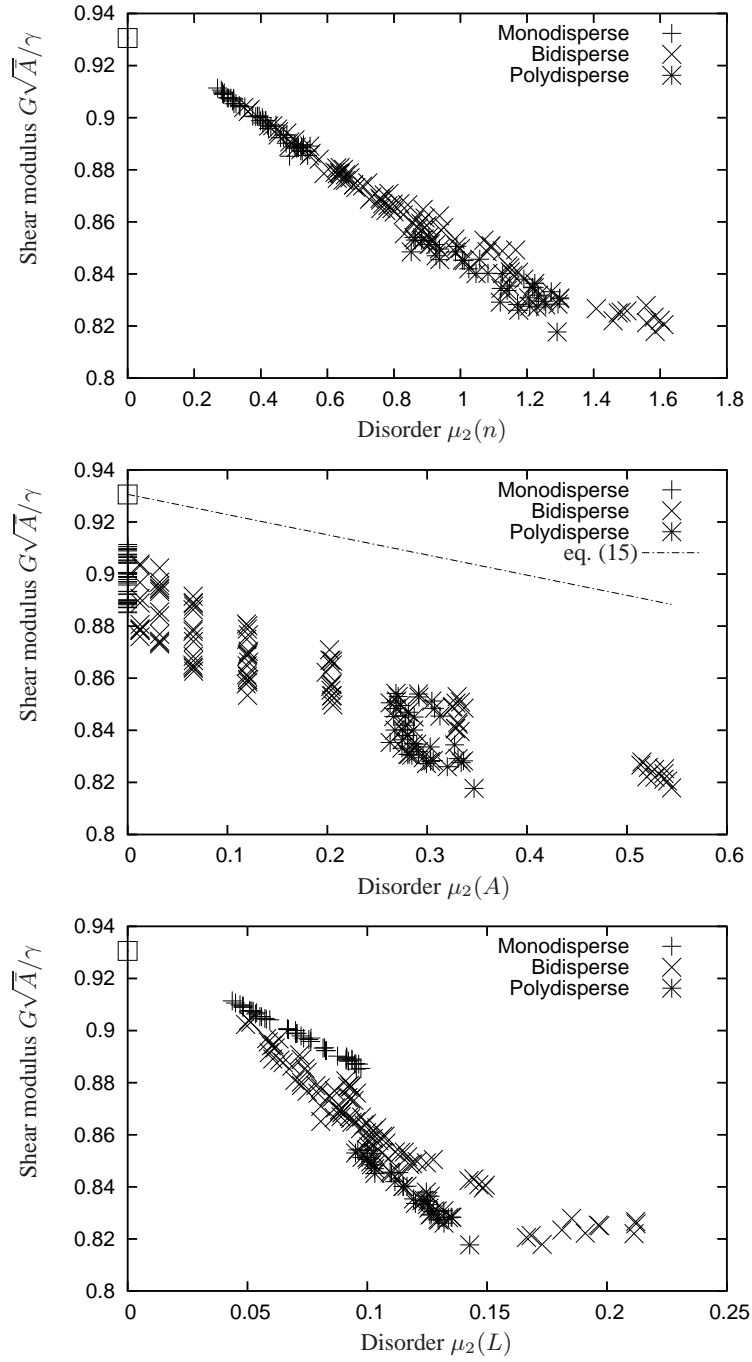


Fig. 6. The shear modulus decreases from the honeycomb value (given by an open square) with increasing disorder in the number of sides n and the edge lengths L . In the case of area disorder, there is an offset at $\mu_2(A) = 0$ before the values of G decrease. Error bars are smaller than the point size and are omitted.

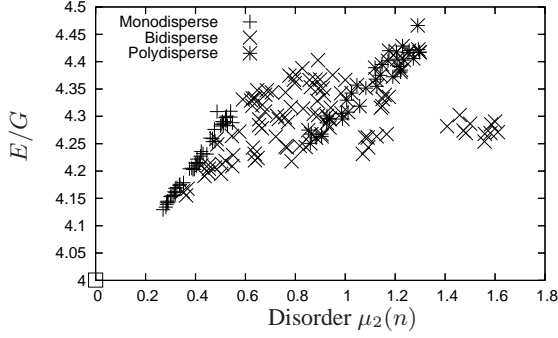


Fig. 7. The ratio of foam energy to shear modulus is about 5 to 10% above the honeycomb value (given by an open square), and increases slightly with increasing disorder in the number of sides n .

tively:

$$G_A = \frac{\gamma}{\sqrt{A}} \sqrt{\frac{2}{3\sqrt{3}}} \left[\frac{1}{2} + \int_0^\infty p(A) \sqrt{\frac{A}{A}} dA \right] \quad (14)$$

$$\approx \frac{\gamma}{\sqrt{A}} \sqrt{\frac{3}{4}} \left[1 - \frac{1}{12} \mu_2(A) \right] \quad (15)$$

$$G_L = \frac{3}{4} \frac{\gamma}{A} \int_0^\infty p(L) \left[\frac{2\bar{L}^2 + L\bar{L} + 3L^2}{2\bar{L} + L} \right] dL \quad (16)$$

$$\approx \frac{\gamma\bar{L}}{A} \frac{3}{2} \left[1 + \frac{2}{9} \mu_2(L) \right] \quad (17)$$

where the approximate forms are for narrow distributions p . In the latter case, the assumption of affine motion means that the shear modulus G_L over-predicts the true value (eq. (17) represents a small correction to the average edge-length data shown in figure 4 multiplied by a factor of 1.5). Eq. (15) is shown on figure 6, where it is also seen to overestimate the shear modulus.

For each foam, we also measure the change in both edge orientation (figure 8) and edge length (figure 9) during the strain step. Note that for an ordered hexagonal foam there is no change in edge orientation under extensional shear parallel to one of the edges. Under simple shear, the three-fold vertices rotate and this is no longer the case.

The change in edge orientation is close to Gaussian (fitting these distributions to a Gaussian gives errors of only a few percent), with negative mean

for shear in the xy direction, positive mean for shear in the yx direction and zero mean for extensional shear. The peak of the distribution is largest for the monodisperse foam. The standard deviation is greater for extensional shear, and the largest values are found for the bidisperse foam with $a_r = 0.3$.

The normalized change in edge length is similar in all three cases, with a symmetric bi-modal distribution; the width of the distribution is approximately twice as great for extensional shear.

5 Summary

We report values of shear modulus G for dry, disordered, 2D foams which are almost isotropic. All results are consistent with a general picture of decreasing shear modulus with increasing disorder. However, a functional form that relates G to the disorder parameters $\mu_2(n)$, $\mu_2(A)$ and $\mu_2(L)$, as well as system wide averages such as that of edge length, \bar{L} , remains elusive.

These disorder parameters are weakly but positively correlated. The average edge length decreases with increasing disorder, except for foams which have regions of hexagonal ordering.

Further complications include the introduction of liquid into the foam, something which is always present in real foams. For low liquid fraction, the results presented here are expected to be appropriate [14], but once the liquid fraction passes a value of about 5%, the shear modulus should decrease as four-sided Plateau borders appear.

Acknowledgements

SJC thanks F. Graner, A. Kraynik, N. Kruyt and D. Weaire for stimulating discussions and advice, as well as participants in the EPSRC-sponsored FRIT conference. ELW was supported by an EPSRC studentship (GR/N28375/01).

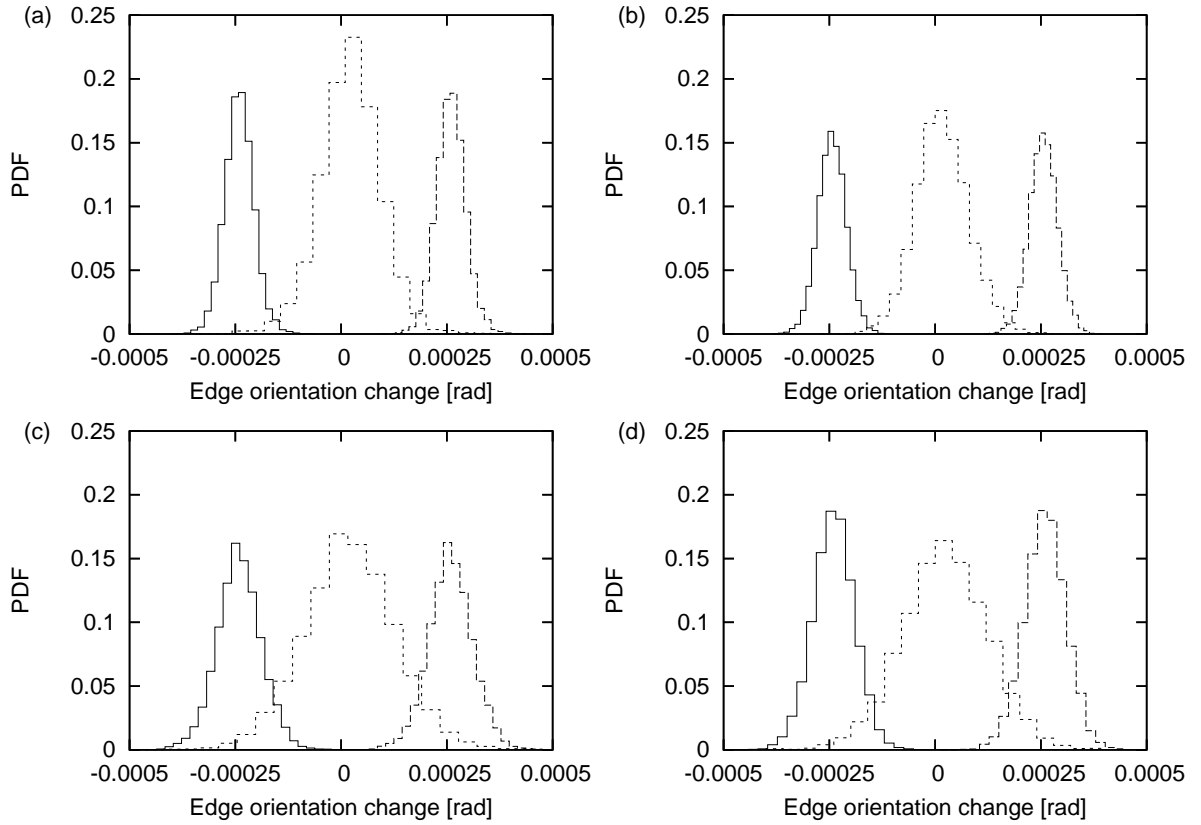


Fig. 8. Representative histograms (21 bins) of the change in edge orientation for simple shear in both xy (solid line) and yx (dashed line) directions and extensional shear in the xx (dotted line) direction. (a) Monodisperse foam. (b) Bidisperse foam with $a_r = 0.7$. (c) Bidisperse foam with $a_r = 0.3$. (d) Polydisperse foam.

References

- [1] D. Weaire and S. Hutzler. 1999 *The Physics of Foams*. Clarendon Press, Oxford.
- [2] H.M. Princen 1969 The Equilibrium Shape of Interfaces, Drops and Bubbles. Rigid and Deformable Particles at Interfaces. In E. Matijević (ed), *Surface and Colloid Science* volume 2. Wiley, New York. pp. 1–84.
- [3] A.M. Kraynik, D.A. Reinelt and H.M. Princen. 1991 The nonlinear elastic behavior of polydisperse hexagonal foams and concentrated emulsions. *J. Rheol.* **35**:1235–1253.
- [4] N.P. Kruyt. 2006 On the shear modulus of two-dimensional liquid foams: a theoretical study of the effect of disorder. *J. Appl. Mech.* **In Press**.
- [5] D. Weaire and M.A. Fortes. 1994 Stress and strain in liquid and solid foams. *Advances Phys.* **43**:685–738.
- [6] D. Weaire, T.-L. Fu and J.P. Kermode. 1986 On the shear elastic constant of a two-dimensional froth. *Phil. Mag. B* **54**:L39–L44.
- [7] A.M. Kraynik, D.A. Reinelt and F. vanSwol. 2003 The structure of random monodisperse foam. *Phys. Rev. E* **67**:031403.
- [8] A.M. Kraynik, D.A. Reinelt and F. vanSwol. 2004 The structure of random polydisperse foam. *Phys. Rev. Lett.* **93**:208301.

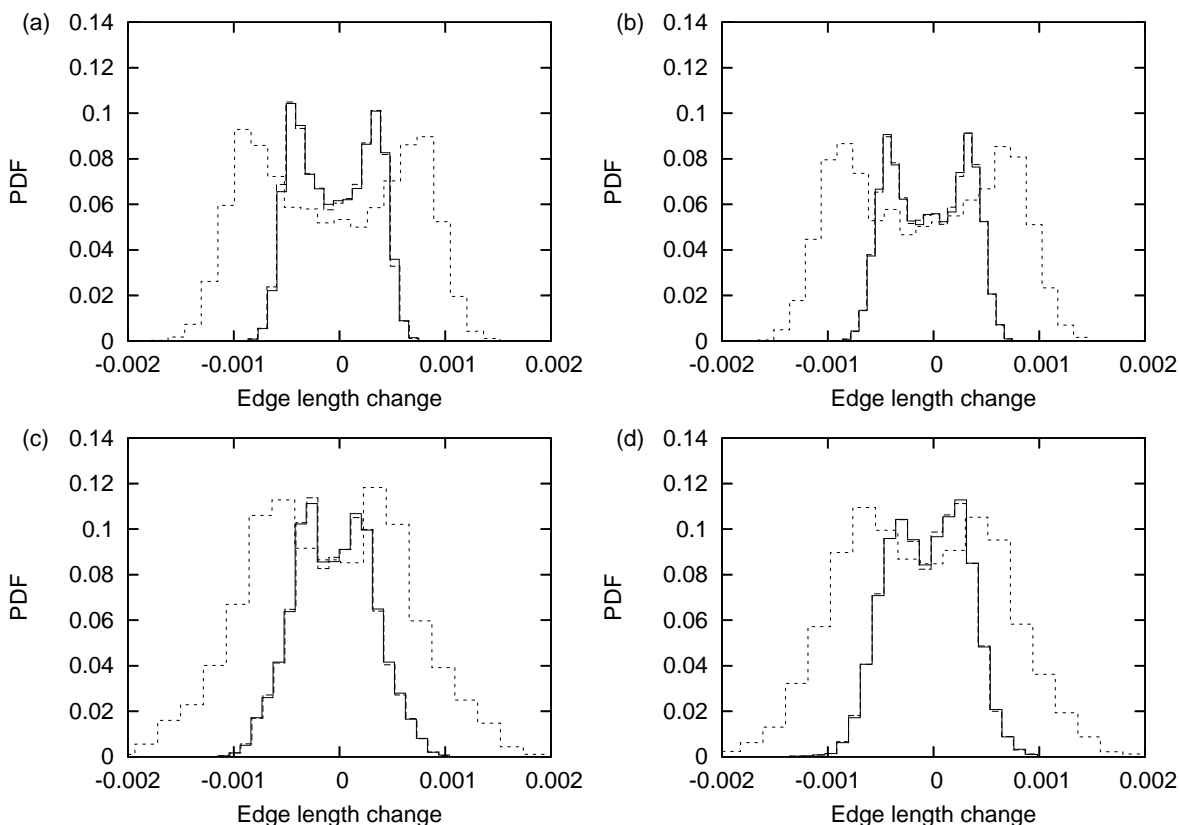


Fig. 9. Representative histograms (21 bins) of change in edge length (normalized by average edge length) with the same key as in figure 8.

- [9] K. Brakke. 1992 The Surface Evolver. *Exp. Math.* **1**:141–165.
- [10] D. Weaire and N. Rivier. 1984 Soap, cells and statistics—random patterns in two dimensions. *Contemp. Phys.* **25**:59–99.
- [11] G.K. Batchelor. 1970 The stress system in a suspension of force-free particles. *J. Fl. Mech.* **41**:545–570.
- [12] F. Graner, Y. Jiang, E. Janiaud and C. Flament. 2001 Equilibrium states and ground state of two-dimensional fluid foams. *Phys. Rev. E* **63**:011402.
- [13] S.A. Khan. 1987 Foam rheology: Relation between extensional and shear deformation in high gas fraction foams. *Rheol. Acta* **26**: 78–84.
- [14] S. Hutzler, D. Weaire and F. Bolton. 1995 The effects of Plateau borders in the two-dimensional soap froth .III. Further results. *Phil. Mag. B* **71**:277–289.